

First Principles Study of Thermoelectric Properties of Skutterudites: $\text{Ir}_4\text{Sb}_{12}$ and $\text{Ca}_{0.04}\text{Ir}_4\text{Sb}_{12}$

B. Bhattarai, T. Dahal, N. P. Adhikari

Journal of Nepal Physical Society

Volume 6, Issue 2, December 2020

ISSN: 2392-473X (Print), 2738-9537 (Online)

Editors:

Dr. Binod Adhikari

Dr. Bhawani Joshi

Dr. Manoj Kumar Yadav

Dr. Krishna Rai

Dr. Rajendra Prasad Adhikari

Mr. Kiran Pudasainee

JNPS, 6 (2), 1-9 (2020)

DOI: <http://doi.org/10.3126/jnphysoc.v6i2.34848>

Published by:

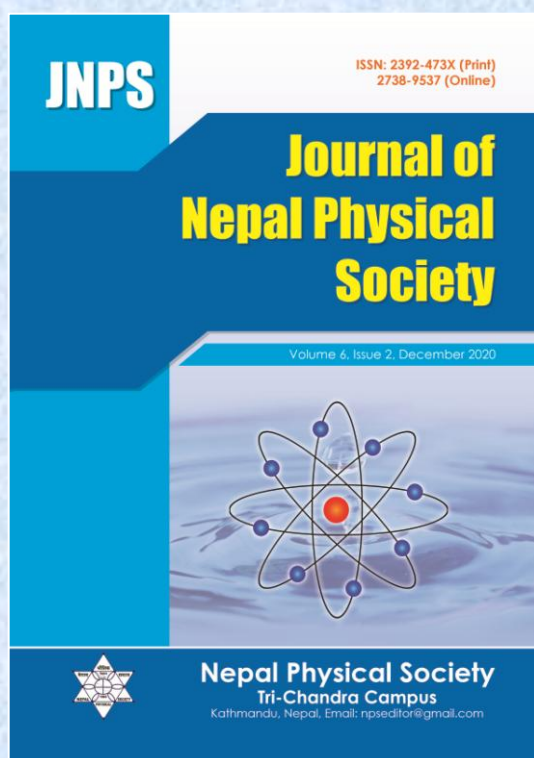
Nepal Physical Society

P.O. Box: 2934

Tri-Chandra Campus

Kathmandu, Nepal

Email: npseditor@gmail.com





First Principles Study of Thermoelectric Properties of Skutterudites: $\text{Ir}_4\text{Sb}_{12}$ and $\text{Ca}_{0.04}\text{Ir}_4\text{Sb}_{12}$

B. Bhattarai¹, T. Dahal², N. P. Adhikari^{1,*}

¹Central Department of Physics, Institute of Science and Technology, T. U., Kathmandu, Nepal

²Austin Community College, Austin, TX 78752

*Corresponding Email: narayan.adhikari@cdp.tu.edu.np

Received: 20 October, 2020; Revised: 29 November, 2020; Accepted: 25 December, 2020

Abstract

First – principles calculations to study thermal and electrical properties of pristine and calcium filled skutterudite $\text{Ir}_4\text{Sb}_{12}$ has been carried out. Density of states (DOS) and band-structure calculations are based on Density Functional Theory (DFT) within Generalized Gradient Approximation (GGA). Transport properties are calculated using BoltzTrap software packages. Volume optimization is carried out on the basis of Murnaghan equation of states. The optimized lattice parameter of pristine $\text{Ir}_4\text{Sb}_{12}$ is found to be 9.4243 Å and that of calcium filled $\text{Ir}_4\text{Sb}_{12}$ is found to be 9.4949 Å. Our calculation shows that pristine $\text{Ir}_4\text{Sb}_{12}$ is a *p*-type of semiconductor with a narrow PBE-GGA band gap of 0.25 eV. After filling calcium, the band gap is reduced to zero showing the metallic behavior of filled compound. Band structure, density of states, variations of electrical and thermal conductivities with temperature and Seebeck coefficient show that calcium filled $\text{Ir}_4\text{Sb}_{12}$ has a metallic character. At Fermi level, the maximum value of thermoelectric figure of merit *ZT* of unfilled $\text{Ir}_4\text{Sb}_{12}$ compound at temperature 400K is found to be 0.5. At the same temperature thermoelectric figure of merit calcium filled $\text{Ca}_{0.04}\text{Ir}_4\text{Sb}_{12}$ is found to be around 0.03. The maximum value of *ZT* of Ca filled $\text{Ca}_{0.04}\text{Ir}_4\text{Sb}_{12}$ at 1000K is computed around 0.1.

Keywords: Seebeck effect, Skutterudites, Thermoelectric figure of merit.

1. INTRODUCTION

The emission of deleterious greenhouse gases by fossil fuels and their limited availability suggest that there is always an ever-growing concern for alternative ‘green’ renewable energy sources and establishment of new efficient technologies of energy conversion [1]. To minimize the dependency on fossil fuels and requirement of high efficiency materials and devices for cooling and power generation, there has been increasing interests in the field of thermoelectric (TE) materials research for a few decades [2,3]. TE materials have potential applications in waste heat recovery because of their ability to achieve reversible conversion between electricity and heat which occurs through electron and phonon propagation [1]. TE materials have been investigated for their use in TE-solar system to

generate power from IR region of the solar spectrum [1, 4, 5].

TE materials are those in which either temperature difference creates an electric potential or application of electric potential creates a temperature difference. Thermoelectric properties of such materials are studied basically on two effects, Seebeck effect and Peltier effect. Devices constructed on the basis of these effects are called thermoelectric devices. They are the solid- state energy converters in which a combination of optimized electrical conductivity, Seebeck coefficient, and thermal properties ensure better energy conversion. TE devices do not have moving parts, are silent, cost-effective, reliable, and environment friendly [4, 6]. These features make TE devices superior over conventional devices.

Efficiency of thermoelectric devices measures the extent at which it converts thermal energy to

electrical energy and vice versa. Mathematically, efficiency of TE devices is given by:

$$\eta_{max} = \frac{\Delta T}{T_H} \frac{\sqrt{1+ZT_{avg}}-1}{\sqrt{1+ZT_{avg}}+\frac{T_C}{T_H}} \dots\dots\dots (1)$$

where, $T_{avg} = \frac{T_C+T_H}{2}$ is the average temperature, T_C = temperature of cold junction, T_H = temperature of hot junction, and $\Delta T = T_H - T_C$ is the temperature difference between hot and the cold junctions. The dimensionless quantity 'ZT' is called thermoelectric figure of merit. It is related to efficiency of TE devices and depends on electrical conductivity (σ), thermal conductivity (κ) and Seebeck coefficient (S) of the material as:

$$ZT = \frac{\sigma S^2 T}{\kappa} \dots\dots\dots (2)$$

where T is the absolute temperature. The thermal conductivity κ , can be written as: $\kappa = \kappa_e + \kappa_l$, where κ_e is thermal conductivity due to electrons and κ_l is the lattice thermal conductivity. Equation (2) suggests that, for a high thermoelectric figure of merit and hence the high device efficiency, the material with high σ , high S , but low κ is needed. Therefore, the material having high electrical conductivity, high Seebeck coefficient and low thermal conductivity is required to make efficient TE devices. One can increase electrical conductivity by increasing the carrier concentration; however this effort will increase the carrier part of thermal conductivity and lower the Seebeck coefficient [7]. The interconnection between electrical conductivity, Seebeck coefficient and thermal conductivity makes the optimization of ZT extremely difficult. One of the ways to optimize ZT comes from reducing the lattice part of thermal conductivity without significantly degrading the electrical conductivity. Since skutterudite is one of the phonon glass electron crystal (PEGC) materials, tuning both electrical conductivity and lattice thermal conductivity simultaneously is a lot easier.

Skutterudites are the compounds having general formula RM_4X_{12} , where R is called filler which may be alkali metal, alkaline earth metal, rare earth metal or actinide, M is the transition metal (Co, Rh or Ir) and X is the pnictogen atom (P, As or Sb) [8]. There are two large voids in each unit cell of skutterudite structure. This structure is ideal for filling guest atom which rattles in the voids thereby

scattering the thermal phonons [3, 8]. Skutterudite compounds have been proven the most promising TE materials because by filling the void in by suitable filler atoms, the lattice thermal conductivity can be effectively reduced. The larger reduction in lattice thermal conductivity results from filling the void by smaller and heavy ions. Smaller is the size of guest atom greater will be the amplitude as well as the frequency of vibration to enhance the scattering of thermal phonon to reduce the thermal conductivity [3]. Heavy guest atoms are effective to transfer the momentum thereby effectively scattering the phonons. The filler atom(s) or the rattler(s) have main two functions. First they donate carriers to host atom to increase the electrical conductivity. Second it rattles about its mean position and hence acts as the phonon scattering center. Both of these conditions are favorable to enhance the dimensionless figure of merit, ZT .

In the present work, we focus on calculating the thermoelectric properties of calcium filled skutterudite. Ir_4Sb_{12} is one of the skutterudite structures and have been proven a promising TE material by various studies [9]. Ir_4Sb_{12} crystallizes in the cubic $Im\bar{3}$ structure, in which Ir and Sb atoms occupy 8c and 24g Wyckoff positions respectively. Each Ir atom is surrounded by six Sb atoms which takes the shape of distorted octahedron leading to a D_{3d} symmetry [10]. Besides, four Sb atoms form rectangles, which are nearly square planar and often termed as Sb_4 rings. These rings orient in such a way that an edge is directed perpendicular to the middle of a plane formed by another Sb_4 rings. The Ir atoms form a primitive cubic sublattice at $(\frac{1}{4}, \frac{1}{4}, \frac{1}{4})$. This structure permits filling dopant at the position (0,0,0) thereby replacing Ir and Sb atom at different ways [10].

2. COMPUTATIONAL DETAILS

We have used two packages viz. WIEN2k and BoltzTrap for the computation of various properties of skutterudite. WIEN2k is an Augmented Plane Wave Plus Local Orbitals (APW + lo) program for calculating crystal properties which is based on Full Potential Augmented Plane Wave (FP-APW) method within Density Functional Theory (DFT) [11]. BoltzTrap is the program which contains **Boltzmann Transport Properties** to calculate the semiclassical transport properties. It is the code for calculating band structure dependent quantities

which is based on the smoothed Fourier interpolation of bands.

For computation, we generated the crystal structure by giving necessary input parameters like atoms present in the crystal, bond length, bond angle, and space group. The initialization involves the calculation of the nearest neighbor distances of atomic spheres, determining the space and point group symmetry, generating the space group symmetry, generating the atomic densities, determining the number of basis functions, and generating the k -mesh in the

Brillouin zone. To calculate the atomic density, we have to specify exchange correlation functional. In the present work, we used PBE-GGA exchange correlation functional for SCF calculations. During SCF calculations we need to be careful about magnetic nature of material. Skutterudite system is non-magnetic therefore it is not necessary to consider spin polarization during SCF calculations. After the completion of SCF, properties like equilibrium lattice constant, cohesive energy, electronic band structure, and density of states are analyzed.

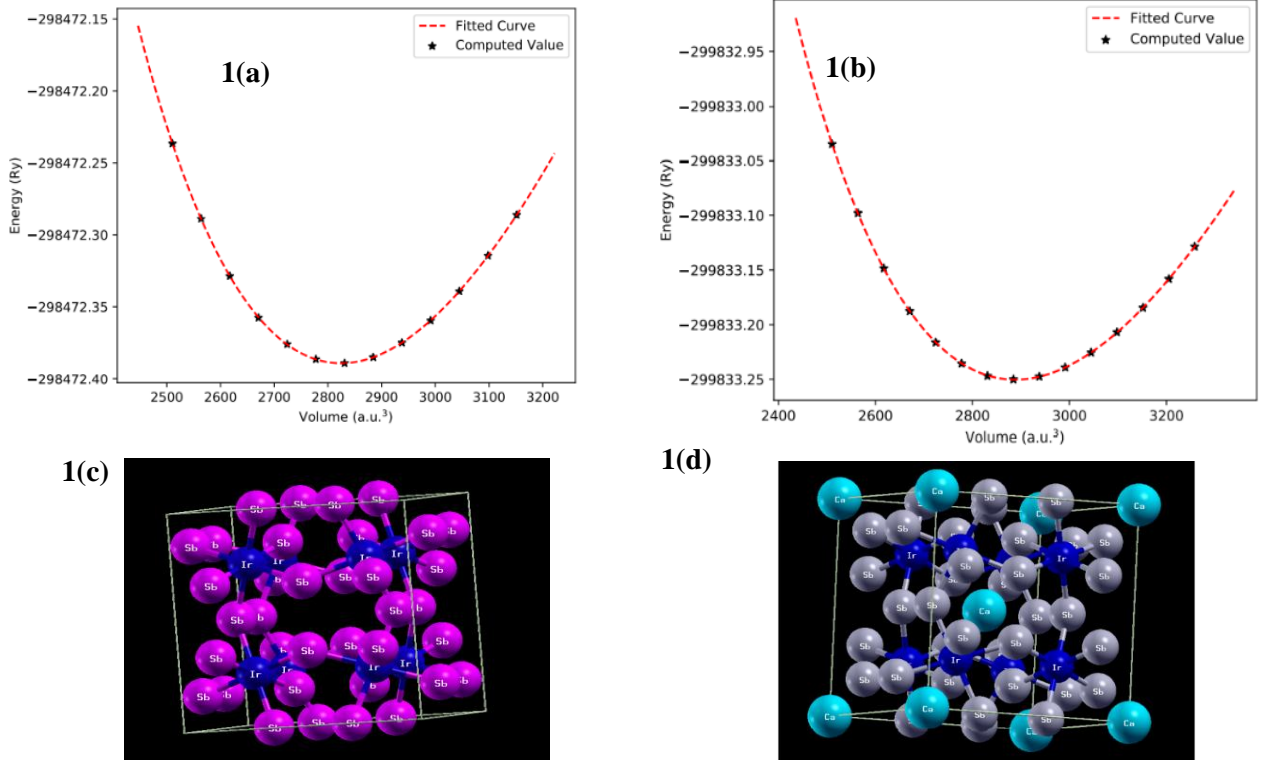


Fig. 1 : (a) Variation of crystal energy with the volume of unit cell of unfilled Ir₄Sb₁₂, (b) Variation of crystal energy with volume of unit cell of Ca filled Ir₄Sb₁₂, (c) and (d) are respectively the unit cell of unfilled and Ca filled Ir₄Sb₁₂.

We have used 15000 k -points in full Brillouin zone corresponding to $24 \times 24 \times 24$ k -points in irreducible Brillouin zone for energy calculations. Energy is stabilized within 10^{-4} Ry for 15000 k -points. Since denser k -mesh is required for density of states and transport properties calculation, we have used 25000 k -points in full Brillouin zone corresponding to $29 \times 29 \times 29$ k -points in irreducible Brillouin zone (IBZ). RK_{max} equal to 7 is used to determine the size of basis set. The radii of Muffin tin spheres, which were calculated by in-built tool of WIEN2k for Ir, Sb and Ca are

respectively 2.44 Å, 2.32 Å and 2.50 Å. The equilibrium volume and the Bulk modulus have been obtained by the use of Murnaghan equation of states. The variation in corresponding energy as a function of volume variation (-10%, -5%, 0%, 5% and 10%) is calculated. We have performed several calculations of the total energy for various unit cell volumes to obtain the value of lattice constant for which total energy is minimum. The value of lattice parameter corresponding to minimum energy is treated as the stabilized lattice constant.

Band structure and density of states (DOS) calculation is based on full-potential (linearized) augmented plane wave ((l) + (APW) + local orbital (lo)) method. The optimized geometry obtained from SCF calculations is used to investigate the structure of crystal lattice. In this program, DOS is calculated by modified tetrahedron method [12]. Figure 1(a) shows the variation of crystal energy with the volume of crystal (in atomic unit) of unfilled $\text{Ir}_4\text{Sb}_{12}$ and figure 1(b) shows the variation of crystal energy with volume for Ca filled compound. Stars represent the calculated points and the dotted line is the best filled Murnaghan equation of state. From the optimized volume, optimized lattice parameters are calculated. The optimized lattice parameter for unfilled $\text{Ir}_4\text{Sb}_{12}$ is found to be 9.4243\AA . For Ca filled $\text{Ir}_4\text{Sb}_{12}$ it is found to be 9.4949\AA . The optimized values of these lattice parameters are used for the further computation of other parameters.

3. RESULTS AND DISCUSSION

A. Crystal Structure and Lattice Parameters

Figures 1(c) and 1(d) shows the unit cells of unfilled $\text{Ir}_4\text{Sb}_{12}$ and Ca filled $\text{Ir}_4\text{Sb}_{12}$ obtained from Xcrysden. It can be seen from the figure that the unit cell of $\text{Ir}_4\text{Sb}_{12}$ has a cage like structure formed by eight Ir atoms in an association with Sb atoms. Guest atom(s) like Ca (present work) can be filled in this void which can vibrate about their mean position thereby scattering the thermal phonons.

Following the method discussed earlier, the calculated optimized lattice parameter of $\text{Ir}_4\text{Sb}_{12}$ is found to be 9.4243\AA . This value lies within 2% of experimental results reported previously by Slack *et al.* (9.2503\AA) [13], Calillat *et al.* (9.2533\AA) [9], and Suzuki *et al.* (9.250\AA) [14]. Similarly, the lattice parameter of $\text{Ir}_4\text{Sb}_{12}$ in the present work is in close agreement with computational result reported by Koga *et al.* (9.445\AA) [15] and Luo *et al.* (9.2498\AA) [16]. The authors in previously reported work [15, 16] have used GGA as exchange correlation functional in their computation.

Table 1: Experimental and computational band gaps of pristine $\text{Ir}_4\text{Sb}_{12}$, showing the effect of exchange correlation functional on the calculated band gap

Band Gap (eV)	Nature of research	Exchange Correlation	Reference
1.18	Experimental	-	[9]
1.4	Experimental	-	[13]

B. Band Structure of Unfilled $\text{Ir}_4\text{Sb}_{12}$

Band structure of unfilled $\text{Ir}_4\text{Sb}_{12}$ is calculated by defining highly symmetric points on the edge of the Brillouin zone. A sampling path of Γ -H-N- Γ -P is used for band structure calculation. The resulting band structure is shown in the figure (2).

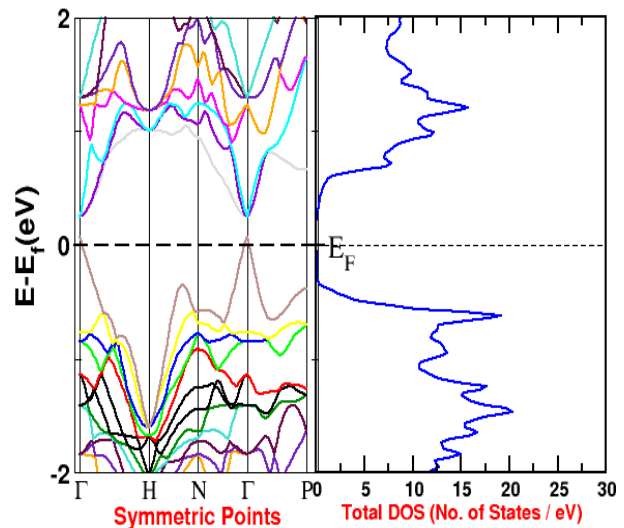


Fig. 2: Electronic band structure and DOS of pristine $\text{Ir}_4\text{Sb}_{12}$ showing the narrow band gap at Fermi level.

Energy values (E) are plotted in reference to the Fermi energy (E_f) therefore the zero value of ($E - E_f$) represents the Fermi level. Our GGA calculation with PBE exchange correlation shows the narrow band gap of 0.25 eV. Sharply defined peaks on the density of states are seen where bands are more crowded. The study of electrical transport properties and thermal transport properties due to carriers in skutterudite is challenging to both, experimentalists as well as theoreticians because of their narrow band gap, complex structure, large unit cell, low symmetry points, and strong covalent bonding [17]. The complexity in electronic properties of such compounds can be seen from large variations in experimental as well as computational band gaps of $\text{Ir}_4\text{Sb}_{12}$ as shown in table (1).

0.075	Computational	LDA	[18]
0.87	Computational	GGA(Tb-mBJ)	[17]
0.086	Computational	GGA(GW)	[17]
0	Computational	GGA (with SO)	[15]
0.25	Computational	GGA(PBE)	Present Work

This large discrepancy in theoretical band gap of binary skutterudite is attributed to the incapability of exchange correlation functional to treat the electrons present in the unit cell of the compound properly. The first important point to note is that, due to covalent nature of bonding in skutterudite, charge leakage occurs to the interstitial regions from the muffin-tin spheres. Therefore, the correct electronic structures of these compounds are not possible for theoretical techniques like LDA, GGA. The discrepancy on the value of band gap resulted from PBE-GGA method in present work is due to large unit cell of the compound ($\sim 9.4\text{\AA}$), large hollow sphere inside the unit cells, narrow symmetry points and strong covalent bonding. For the correct calculation of electronic properties, most of the electrons of the system should reside within the muffin tin spheres so that the effective crystal wavefunction includes contribution from most of the electrons. This condition is not possible in skutterudite due to large unit cell and empty site inside the cell. It is therefore, the calculation using LAPW method could not reproduce good result regarding band structure and band gaps. Further, it is found that a small variation in lattice parameters affect the computational band gap of skutterudites.

C. Band Structure Ca filled $\text{Ir}_4\text{Sb}_{12}$

The electronic band structure and DOS of calcium filled $\text{Ir}_4\text{Sb}_{12}$ is shown in figure (3). It is clear from figure (3) that, although bottom of the conduction band around the gap is relatively flat as compared to the band structure of unfilled $\text{Ir}_4\text{Sb}_{12}$, the top of valance band still exhibits strong dispersive character near the Γ point. Near Γ point, band still retains Ir d and Sb p character. The bottom of the conduction band is dominated by the s -band driven from filler (i.e from Calcium), everywhere except near Γ point. Those bands which were previously in conduction band are now present in valance band. DOS clearly indicates that there is non-zero density of states at Fermi level. Intrinsic $\text{Ir}_4\text{Sb}_{12}$ is p -type semiconductor while filling the void Ca turns it into a metallic system by giving electrons to the crystal matrix. Our calculation shows that Ca filling have

little effect on the near-edge DOS of $\text{Ir}_4\text{Sb}_{12}$, except moving the Fermi level up to the conduction band. The result obtained is in good agreement with the previous work with similar kind of fillers [19].

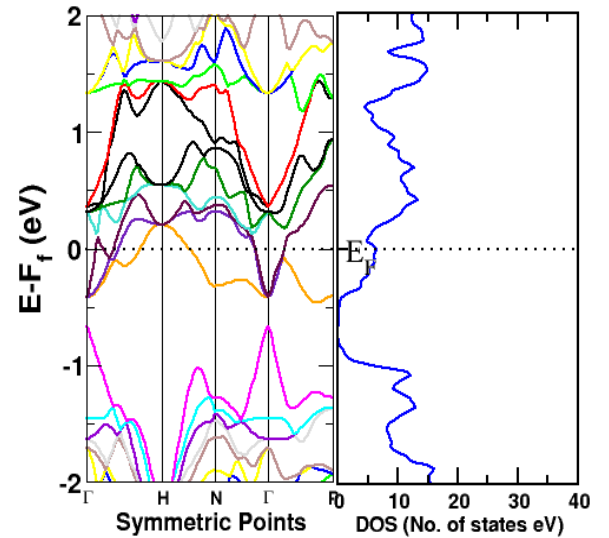


Fig.3: Electronic band structure and DOS of Ca filled $\text{Ir}_4\text{Sb}_{12}$ showing the shifting of Fermi level up towards the conduction band after filling Ca.

D. Density of States of unfilled $\text{Ir}_4\text{Sb}_{12}$

While making graphs for DOS, total number of states per unit energy range (in eV) is plotted along Y-axis and corresponding energy (eV) is plotted in X-axis with reference to the Fermi energy.

In figure 4(a) the solid line represents the total DOS which is the sum of DOS of each Ir and Sb atoms at corresponding energy value. Hybridization of $5d$ orbitals of Ir and $5p$ orbitals of Sb results in the small band gap of an about 0.25 eV. Figure 4(a) shows that Ir has significant contribution in total DOS in valance band whereas in conduction band the contribution of Sb is relatively more.

In Sb maximum in total DOS comes from $5p$ orbitals (Fig. 4b). This is due to the partially filled $5p$ orbital of the valance band of Sb. Similarly, in Ir there is a partially filled $5d$ orbital in valance shell. Therefore, the contribution to total DOS due to $5d$ orbital is significant among other orbitals, as shown in figure 4(c).

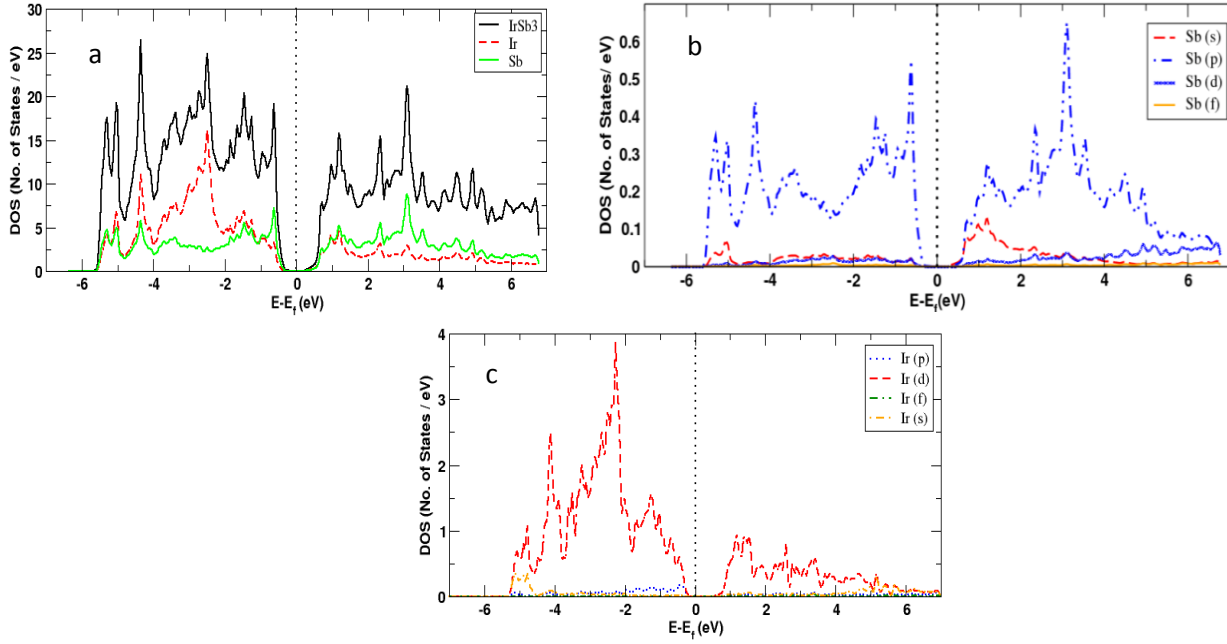


Fig. 4 : (a) Total DOS of $\text{Ir}_4\text{Sb}_{12}$ showing Ir and Sb contributions, (b) Contributions of different orbitals of Sb and (c) contribution of different orbitals of Ir on total DOS of $\text{Ir}_4\text{Sb}_{12}$

E. Density of States of Ca filled $\text{Ir}_4\text{Sb}_{12}$

After filling calcium, several changes in DOS of the compound are noticed. They are individually presented in figure 5(a) to 5(d). Figure 5(a) shows the contribution of individual atoms in the total DOS of Ca filled $\text{Ir}_4\text{Sb}_{12}$. It can be noticed that, the contribution of Ca is almost zero in valance band but it's contribution is relatively more in the conduction band. The maximum

value of DOS of the compound has been increased after filling calcium. Figure 5(b) shows, the significant contribution of Ir, p orbital in the total DOS of the system. Similarly, as seen from figure 5(c), $5p$ orbitals of Sb is contributing more to the total DOS. The maximum contribution of calcium d orbital (fig. 5d) in conduction band is the reason of metallic character of the filled skutterudite.

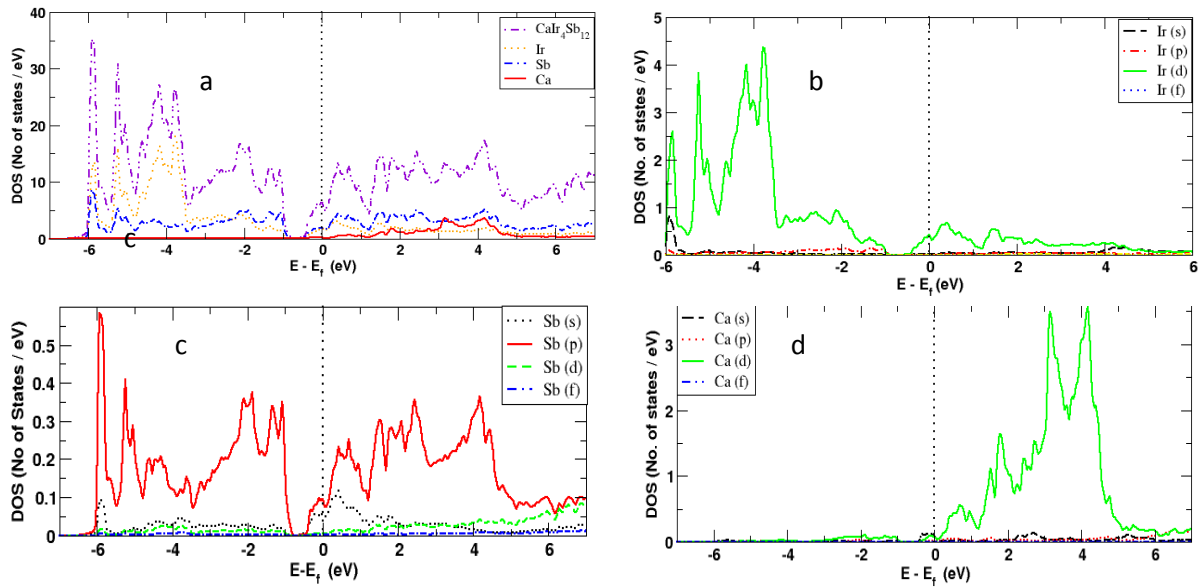


Fig. 5 : (a) Total DOS of $\text{CaIr}_4\text{Sb}_{12}$ showing Ir, Sb and Ca contributions, (b) contributions of different orbitals of Ir, (c) contribution of different orbitals of Sb, (d) contributions of different orbitals of Ca, on total DOS of $\text{CaIr}_4\text{Sb}_{12}$

F. Effect of filler in transport properties

Depending on the nature of dopant, doping always results in changing various properties of material. Figure (6) shows the variation of thermal carrier conductivity per relaxation time (κ_e/τ) with temperature for both, unfilled and Ca filled $\text{Ir}_4\text{Sb}_{12}$.

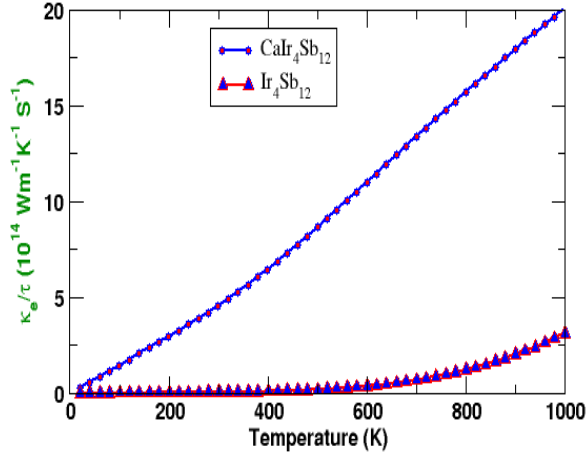


Fig. 6: Variation of electronic thermal conductivity (per relaxation time) of unfilled and Ca filled $\text{Ir}_4\text{Sb}_{12}$ with temperature

The variation of thermal conductivity with temperature of unfilled $\text{Ir}_4\text{Sb}_{12}$ is non-linear (fig. 7). This indicates the semiconducting nature of p -type $\text{Ir}_4\text{Sb}_{12}$. However, the linearity in the graph of thermal conductivity vs. temperature of filled compound suggests its metallic behavior ($\kappa_e = \frac{\pi^2 n k_B T \tau}{3m}$). It can be concluded that Ca filling turned the compound from p -type semiconductor to a metallic compound.

Similarly, the variation of electrical conductivity per relaxation time (σ/τ) with temperature of both materials is shown in figure (7). The graph shows that, electrical conductivity increases significantly after filling calcium. It is due to the transfer of free electrons from calcium to the host atom. For metals the ratio $\frac{\sigma}{\tau} = \frac{ne^2}{m}$ is approximately constant. The constancy in this ratio can be seen in the graph showing variation of $\frac{\sigma}{\tau}$ with temperature of Ca filled $\text{Ir}_4\text{Sb}_{12}$. This result further supports the metallic nature of Ca filled $\text{Ir}_4\text{Sb}_{12}$. However, in semiconductor, increase in temperature increases the carrier concentration so electrical conductivity increases. There is an exponential increase in $\frac{\sigma}{\tau}$ with temperature for unfilled $\text{Ir}_4\text{Sb}_{12}$.

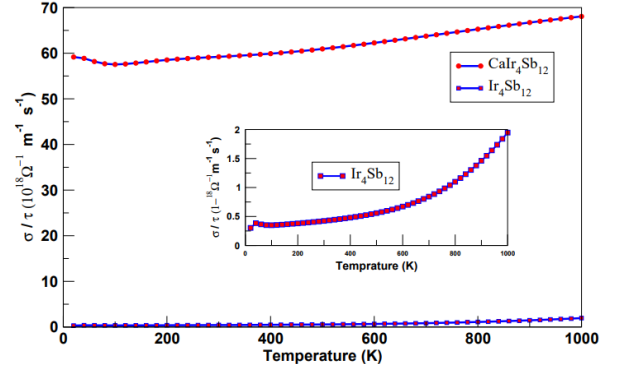


Fig. 7: Variation of electrical conductivity (per relaxation time) of unfilled and Ca filled $\text{Ir}_4\text{Sb}_{12}$ with temperature

The variation of Seebeck coefficient with temperature is represented in figure (8). The positive value of Seebeck coefficient of unfilled compound suggests its p -type nature. After doping calcium, the sign of Seebeck coefficient has been changed from positive to negative, suggesting electrons as majority charge carriers (fig. 8). The Seebeck coefficient of unfilled compound increases with temperature and attains the maximum value of about $175 \mu\text{V}/\text{K}$ around 780K . This result is in close agreement with previously reported value by T. Calliet *et al.*[9]. The decrease in Seebeck coefficient of unfilled compound after 780K with temperature may be due to the bipolar conduction of minority charge carriers. The maximum value of Seebeck coefficient can be used to estimate the band gap of thermoelectric materials using the relation: $E_g = 2eS_{max}T_{max}$ [20]. From this relation we calculated the band gap of $\text{Ir}_4\text{Sb}_{12}$ to be around 0.27 eV . This value lies within 10% of the calculated value 0.25 eV .

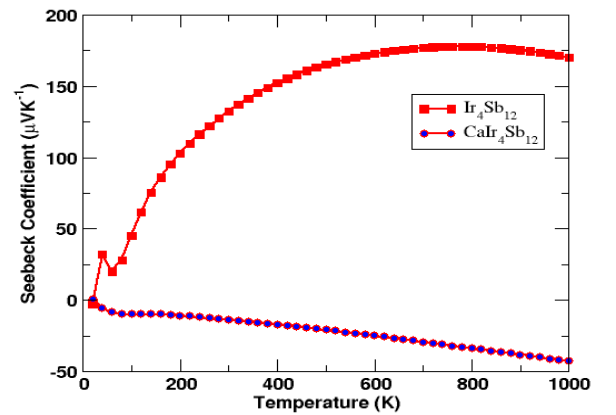


Fig. 8: Variation of Seebeck coefficient of unfilled and Ca filled $\text{Ir}_4\text{Sb}_{12}$ with temperature

Effect of calcium filling on the quantity $\frac{S^2\sigma T}{\kappa_e}$ (ZT without lattice contribution) of $\text{Ir}_4\text{Sb}_{12}$ has been studied. The graph between $\frac{S^2\sigma T}{\kappa_e}$ versus temperature is plotted and presented in figure (9). If we add the phonon contribution (κ_l) to the (κ_e) in the quantity $\frac{S^2\sigma T}{\kappa_e}$ then it gives thermoelectric figure of merit ZT . In other words, the quantity $\frac{S^2\sigma T}{\kappa_e}$ represents the dimensionless thermoelectric figure of merit ZT without lattice contribution. Figure (9) shows that the value of quantity $\frac{S^2\sigma T}{\kappa_e}$ increases monotonically for filled compound. For unfilled compound, it increases continuously, attains a maximum value of 0.5 at around 400K and then decreases. Without considering the lattice contribution, the value of quantity $\frac{S^2\sigma T}{\kappa_e}$ of calcium filled skutterudite is obtained around 0.1 at 1000K which is far less than the corresponding maximum value of unfilled compound. However, optimization of Ca and Ir concentration may result in the improvement of the value of $\frac{S^2\sigma T}{\kappa_e}$.

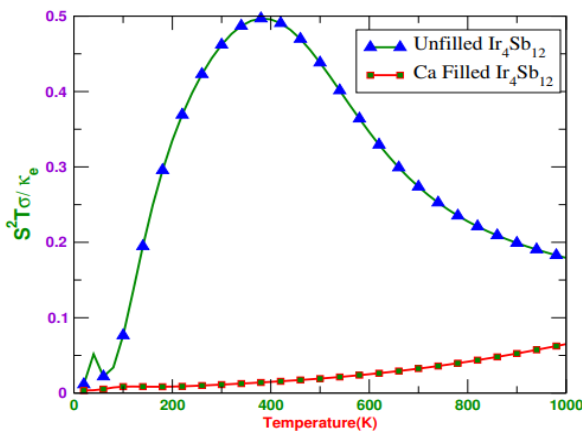


Fig. 9: Variation of the quantity $\left(\frac{S^2\sigma T}{\kappa_e}\right)$ of unfilled and Ca filled $\text{Ir}_4\text{Sb}_{12}$ with temperature

CONCLUSIONS AND CONCLUDING REMARKS

The equilibrium lattice constant of $\text{Ir}_4\text{Sb}_{12}$ and of Ca filled $\text{Ir}_4\text{Sb}_{12}$ has been found to be 9.4243 Å and 9.4949 Å, respectively. The computed value of band gap of unfilled $\text{Ir}_4\text{Sb}_{12}$ is found to be 0.25 eV. The positive Seebeck coefficient at all the temperature values indicates that $\text{Ir}_4\text{Sb}_{12}$ is a p -type

semiconductor compound. Filling of calcium atom on the voids of the structure shifted the Fermi level towards the conduction band and resulted a band gap equal to 0 eV. Due to the increase in thermal conductivity and decrease in Seebeck coefficient, the dimensionless figure of merit ZT of Ca filled skutterudite underperformed compared to unfilled compound. The maximum value of $\frac{S^2\sigma T}{\kappa_e}$ is around 0.1 for calcium filled $\text{Ir}_4\text{Sb}_{12}$ at around 1000K. This suggests Ca might not be good candidate for enhancing thermoelectric figure of merit of the compound at filling fraction of 0.04. However the authors are planning to extend this work further by changing the Ca concentration to optimize the value of ZT of the filled compound.

ACKNOWLEDGEMENT

We acknowledge University Grants Commission for the financial support. We express our sincere gratitude to the Central Department of Physics, Tribhuvan University.

REFERENCES

- [1] Li, Z.; Xio, C.; Zhu, H. and Xie, Y. Defect Chemistry for Thermoelectric Materials. *J.A. Chem. Soc*, **138**: 14810-1419 (2016).
- [2] Nolas, G. S.; Morcelli, D. T.; Tritt, T. M. Skutterudite: a phonon glas electron crystal approach to advanced thermoelectric energy conversion applications. *Ann. Rev. Mater*, **29**: 89 (1999).
- [3] Dahal, T.; Kim, H. S.; Gahlwat, S.; Dahal, K.; Jie, Q.; Liu, W.; Lan, Y.; White, K. and Ren, Z. Transport and mechanical properties of the double- filled p -type skutterudite $\text{La}_{0.68}\text{Ce}_{0.22}\text{Fe}_{4-x}\text{Co}_x\text{Sb}_{12}$. *Actamaterialia.*, **117**: 13-22 (2016).
- [4] Bell, L.E. Cooling, heating, generating power and recovering waste heat with thermoelectric systems. *Science*, **321**: 1457 (2006).
- [5] Tritt, T. M.; Bottner, H. and Chen, L. D. Thermoelectrics: direct solar thermal energy conversion. *MRS Bull*, **33**: 366 (2008).
- [6] Kurosaki, K.; Li, G.; Ohishi, Y.; Muta, H. and Yamanaka, S. Enhancement of thermoelectric efficiency of CoSb_3 -based skutterudites by double filling with K and Tl. *Front. Chem.*, **2**: 84-88 (2014).
- [7] Synder, G. H.; Toberer, E. S. Complex Thermoelectric materials. *Nature materials*, **7**: 105-109 (2008).
- [8] Dahal, T.; Jie, Q.; Liu, W.; Dahal, K.; Guo, K.; Lan, G. and Ren, Z. Effect of triple fillers in thermoelectric performance of p -type

- skutterudites *Journal of Alloys and Compounds I*, **623**: 104-108 (2015).
- [9] Calillat, T.; Borchchevesky, A. and Fleurial, J. P. Preparation and Thermoelectric properties of p-type and n-type IrSb₃. *AIP Conf. Proc.* **316**: 31-35 (1994).
- [10] Hammerschmidt, L.; Schlecht, S. and Paulus, B. Electronic Structure and the ground-state properties of cobalt antimonideskutterudites: Revisited with different theoretical methods. *Phys. Status. Solidi A*, 1-9 (2012).
- [11] Blaha, P.; Schwarz, K.; Madsen, G. K. H.; Kvasnika, D. and Luitz, J. *An augmented plane wave + local orbitals program for calculation crystal properties* (2001).
- [12] Blochal, P. E.; Jepson, O. and Anderson, O. K. Improved tetrahedron method for Brillouin-zone integrations. *Physical Review*, **49**: 16223-16225 (1994).
- [13] Slack, G. A. and Tsoukala, V. G. Some properties of semiconducting IrSb₃. *J. Appl. Phys.* **76**: 1665-1670 (1994).
- [14] Suzuki, T.; Kikkawa, A.; Tokura, Y. and Taguchi, Y. Impact of electron doping on thermoelectric properties in filled skutterudite IrSb₃. *Phys. Rev. B*, **93**: 155101 (2016).
- [15] Koga, K.; Akai, K.; Oshiro, K. and Matsuura, M. Electronic structure and optical properties of binary skutterudite antimonides. *Phys. Rev. B*, **71**: 155119 (2005).
- [16] Luo, H.; Krizan, J. W.; Muechler, L. *et al.* *Nature Communications*, **6**: 6489-6493 (2015).
- [17] Khan, B.; Aliabad, M.; Ghazanfari, M. and Ahmad, I. Electronic band structures of binary skutterudite. *Journals of Alloys and Compounds*, **647**: 364-369 (2015).
- [18] Takegahara, K. and Harima, H. Systematic study of electronic band structures for binary skutterudite compounds. *Physica B: Condensed Matter*, **328**: 74-76 (2003).
- [19] Mei, Z. G.; Yang, J.; Pei, Y. Z.; Zhang, W. and Chen, L. D. Alkali metal filled CoSb₃ skutterudites as thermoelectric materials: Theoretical study. *Phys. Rev. B*, **77**: 045202-045205 (2008).
- [20] Zachary, M. G.; Hyun, S. K.; Heng, W. G. J. S. Band gap estimation from temperature dependent Seebeck measurement – deviations from the $2eS_{max}T_{max}$ relation. *Appl. Phys. Lett.* **106**: 022112 (2015).